PELVIS BONE FRACTURE MODELING IN LATERAL IMPACT

Eric Song
Laurent Fontaine
Xavier Trosseille
Hervé Guillemot
LAB PSA Peugeot-Citroën Renault
France
Paper Number 05-0247

ABSTRACT

This paper presents personalized simulations of eleven isolated pelvic bones under lateral impact and a generic 50th percentile male pelvic bone model based on these simulations. Eleven pelvises were solicited by metallic spheres in the acetabulum, which were impacted by a falling mass of 3.68 kg at a speed of 4 m/s. Each pelvis test was then modeled individually, taking into account its proper geometry and mass. Damageable material law was used to simulate the bone stiffness and fracture. For each pelvis test were determined equivalent elastic modulus, yielding stress and damage plastic strain representing combined contributions of material properties and cortical bone thickness to pelvis bone resistance. Based on these personalized simulations a generic 50th percentile male pelvic bone model was defined and integrated into a full body model to simulate cadaver tests on pelvis where bone fractures were documented. Three material laws were then identified and associated with this model, representing respectively a fragile, a medium and a resistant pelvis bone. The mechanical behavior of this pelvis model was also compared to experimental data on cadavers. It showed that the pelvis model developed is globally relevant with respect to experiments in terms of pelvis loading prediction, this for a large range of impact energy from 130 to 1150 Joules. This paper provides new data and insights for pelvis bone fracture modeling in lateral impact. The resulted model is consistent with available impactor test data on pelvis and constitutes a useful tool for lateral impact injury research.

INTRODUCTION

Side impacts represent 15 to 20% of the automotive collisions in which at least one of the occupants was injured but are the cause of 25 to 30% of serious and fatal injuries encountered in all car accidents. Protection of occupants in side impact remains a big challenge despite of progress made in the past years. In fact the very limited space between car door and occupant make very difficult to dissipate the engaged impact energy in a smooth manner. In order to optimize protection strategy and to improve protection equipments more biomechanical knowledge is needed on pelvis tolerance of different population groups, for example, a vulnerable 50th percentile male.

The pioneer work of Césari *et al.* [1980, 1982] led the basis for pelvis loading based injury criterion definition. 55 cadaver tests on 22 subjects were performed by impacting the great trochanter with a spherical rigid impactor. Césari concluded that the value of tolerance in terms of impact force is close to 10 kN for a time period of 3ms for the 50th percentile male subjects and close to 4 kN for the 5th percentile female. However it is to be noted that less than 30% of subjects tested have mass included between 77±10kg. Moreover, average age of subjects tested rises to 70 years.

More impactor tests on pelvis have been performed and published ever since. Viano [1989] performed 10 cadaver tests with a circular but flat impactor of 23.4 kg. Subjects tested were relatively younger than those of Césari. Tolerance in terms of impact force revealed to be higher. Bouquet *et al.* [1994] performed cadaver tests also with an impactor of 23.4 kg. The impact surface was nevertheless a rectangular rigid plate of 200x100 mm^2. They showed a lower tolerance level in terms of impact force: around 8 kN. Bouquet *et al.* [1998] performed more cadaver tests but with a larger impact surface (200x200 mm) in order to include the contribution of iliac wing. Impactor mass and impactor velocity were designed in such a way so that they can examine which one, between mass and velocity, is dominant for a given energy level. In fact they found that to represent car crashes, the impacting masses should be lower than the famous 23.4 kg impactor, and considered essential to know the pelvis behavior in new impact conditions. Based on their new cadaver tests, they concluded that for a given impactor energy, neither its mass nor velocity seemed to be dominant.

Side impact dummies were evaluated with respect to some configurations of above cadaver tests. Both SID and EuroSID were demonstrated to have a too stiff pelvis with respect to cadaver responses. WorldSID shows more close responses. However its load path showed big difference with respect to EuroSID when comparing symphysis contribution to total loading sustained by pelvis. It is important to understand the mechanism of force path and to determine the consequence of these differences when dummies are used to develop protection systems.

Also to define injury criteria thresholds, it is usual to normalize cadaver test responses while keeping always the same injury outcome. No elements were showed to support such an approach.

A mathematical model of the pelvis, capable of injury prediction, should constitute a valuable tool to address the different problems listed above.

Numerous models of pelvis can be found in the literature. Many of them were developed to simulate the pelvis behavior during the walk cycle or to study the interaction of the pelvic bone with hip prosthesis [Goel *et al.*1978; Oonishi *et al.*1983; Dalstra *et al.*1993, 1995]. Models dealing with pelvis behavior and injuries under car related impact conditions remain a minority.

Chamouvard *et al.* [1993] developed a spring-mass model of pelvis for lateral impact. However, it was limited to give only a global response in terms of force, displacement, or acceleration, in mono-axial conditions. Renaudin *et al.* [1993] developed a finite element model of pelvis. Considering that the trabecular bone had a low influence in terms of overall stiffness of the pelvis [Dalstra *et al.* 1993], they represented pelvis bone by only shell elements, corresponding to the external surface of the structure. The model was designed from a metallic model of the 50th percentile of Reynolds. Moreover, thickness from 1 to 4 millimeters, measured on experimented pelvis, were attributed to the shell elements. Nodal masses were distributed to correspond to the global characteristics of a pelvis. The Young's modulus in this model was low, around 3000 MPa. Static tests [Guillemot *et al.*1995] were first conducted under side loading conditions, in order to validate this model. Besnault *et al.* [1998] improved this model by adding geometrical parameters to adapt it to different tested bones, using a kriging technique. Plummer *et al.* [1996] proposed a modified version of a model of Bidez, built from CT scan slices, which aimed at the study of pelvis fracture etiology, in the context of automotive side impact conditions. Nevertheless, this model did not represent a whole pelvis: a coxal bone was modeled, but the sacrum and the contralateral ilium were not taken into account. Finally the acetabulum was fitted with a hip prosthesis. Dawson *et al.* [1998] proposed a model, also dedicated to lateral impacts in the field of car accidents. The model was created from 74 CT scan slices, and distorted by scale factors to correspond to the 50^{e} percentile of Reynolds. The two coxal bones and the sacrum were built by 8-node elements, and connected to each other by 32 springs for the sacro-iliac joints and 8 springs for the pubic symphisis. Joint properties were established from the literature [Fung 1965; Mak 1986]. Bone characteristics were given element by element, from CT scan density levels, and range from 250 to 1500 MPa for the trabecular bone Young's modulus. The meshing included 1511 8-node elements and 3769 nodes. The complete model was validated by using a modal analysis. However, the pelvis mass (0,534 kg) is lower than a real one.

In spite of numerous models reviewed above, there is still a need of a pelvis model, capable of simulating pelvis bone fracture in lateral pelvis impact, relevant with respect to currently available cadaver impactor test data, and sufficiently validated to represent human pelvis behavior and its variation versus different groups of car occupant population.

This paper intends to develop such a model. Based on the work performed by Besnault *et al.* [1998], where was developed a kriging technique and allows taking into account particular geometry of each pelvis simulated, 11 impactor tests on isolated pelvis bone have been individually simulated and corresponding mechanical properties and its range of variation determined. Then a generic model of pelvis was constructed and integrated to a whole human body model [Lizée *et al.* 1998]. With this model, impactor tests on cadavers presented above were simulated and material laws derived to represent different levels of resistance due to individual variation. Finally model responses were evaluated with respect to impactor test data.

MODEL DEVELOPMENT

Geometry

The reference FE mesh of pelvis bone (See Figure 1 represents the shape of a 50th percentile male.

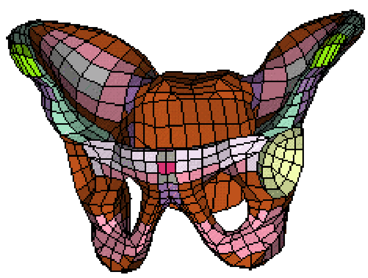

Figure 1. Reference FE mesh of pelvis bone representing the shape of a 50th percentile male.

This shape was based on the data of Reynolds *et al.* [1981]: their statistical study concerning 3000 pelvic bones of north Americans has allowed the design of a pelvis casting corresponding to the 50th percentile male. This pelvis casting was digitalized and then meshed by shell elements to represent cortical bone. Trabecular bone was not taken into account in reason of its low influence on overall stiffness of pelvis. The two acetabula, missing in the casting, were included by two spherical segments positioned at each hip centre.

Stiffness and fracture of pelvis bone are conditioned by thickness of its cortical bone. Examination of five pelvis bone [Guillemot 1992] showed considerable variation of thickness from one location to another: it passes from several tenths millimeter in the centre of iliac wing to nearly 4 mm for the iliac spine. This variation clearly suggests that it is not relevant to use a uniform thickness repartition through pelvis bone, in particular when cortical bone fracture simulation is aimed at, since yielding and rupture occurrence of a plate is directly linked to its thickness for a given local loading. To take into account this variation of thickness through pelvis bone, each element was attributed a thickness according to its position based on data obtained from these five pelvises.

Mechanical properties

Few experimental data are available on pelvic bone. Only data found were given by Kuhn and Goldstein [1989] on iliac crest, with an elastic modulus varying between 3.0 and 5.3 GPa. In this study our objective was to develop a pelvis model with bone fracture simulation. To do this, an elastoplastic law with damage was attributed to cortical bone. As showed by Figure 2, the parameters of this law are the elastic modulus, the elastic threshold, the maximum stress and the damage plastic strain.

Due to the lack of experimental data on these parameters for pelvis cortical bone, Guillemot tests on isolated pelvis [1997] were used: the simulation of these tests should allow estimating these parameters.

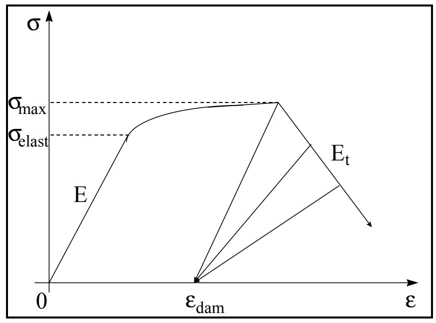

Figure 2. Elastoplastic material law with damage (Radioss-Mecalog).

However we know that pelvis bone stiffness and fracture are conditioned by thickness of pelvis bone. So it is no use focusing on real material parameters for simulating an individual pelvis while the thickness and its repartition are unknown.

The following approach was adopted for the definition of mechanical properties: thickness and its repartition remain constant from one pelvis to another while the elastic modulus, the elastic threshold, the maximum stress and damage plastic strain vary to present dispersion of pelvis bone across occupant population. It means that these mechanical parameters should be considered as equivalent ones which assume, together with cortical bone thickness, similitude between the model and corresponding pelvis simulated in terms of dynamic responses and injury outcome for considered configuration.

Although few experimental data are available on pelvis bone, many experiments have been done on long bone, in particular on femur and tibia. Review of these experiments by Viano [1986] showed that cortical bone can undergo yielding up to 3-4% before ultimate failure and elongation above 0.5% strain generally causes microstructure damage in the material and inelastic behaviour. Table 1 is an example of experimental data obtained by Burstein *et al.* [1976] for tibia tensile properties, and indicates that: 1) the ratio σy/E is around 0.5%; 2) the difference σu – σy is around 28 MPa

Table 1.
Tensile properties of tibia for different age groups according to experiments of Burstein *et al.*

Age (yrs)	E (MPa)	σy (MPa)	σu (MPa)	σy/E	σu-σy (MPa)
20-29	18900	126	161	0,0067	35
30-39	27000	129	154	0,0048	25
40-49	28800	140	170	0,0049	30
50-59	23100	133	164	0,0058	31
60-69	19900	124	147	0,0062	23
70-79	19900	120	145	0,0060	25
80-89	29200	131	156	0,0045	25
Moyen	23829	129	157	0,0054	28

Based on these literature data, further specifications were added to the target material law of cortical bone of pelvis:

σy = 0.005*E
σu – σy = 30 MPa
εp = 3%

In order to determine the magnitude of these mechanical parameters, simulations of experiments on isolated pelvis bone were performed, giving thus a first estimation of E, σy, σu and εp.

Simulations of tests on isolated pelvis bone

Guillemot *et al.* [1997] performed dynamic tests on isolated pelvis bone. 11 pelvis bones were extracted from fresh cadavers. A drop tower was used to impact these bones. It consisted of a falling mass guided between two rails which enables impact speeds up to 4 m/s. Each pelvis was fixed up to the external edge of the left ischial tuerosity. A falling mass of 3.68 kg impacted a metallic ball fitted into the right acetabulum which distributes the load all around the joint surface.

Besnault *et al.* [1998] developed an automatic procedure in order to adapt a unique reference FE mesh to different morphologies. This procedure was based on the Kriging technique and a study on pelvis geometry with determination of characteristic dimensions. With this procedure, the reference FE mesh was transformed into the morphology of each pelvis bone tested while thickness and its repartition were kept unchanged between different pelvises. The mass density was adjusted in order to get the mass of the simulated pelvis bone. The model was loaded by imposing the displacement of the ball, according to experiment recording. The reaction force of the pelvis bone was compared to the experimental measurement to determine the appropriate parameters.

Figure 3 shows an example of simulation for the test 9707.

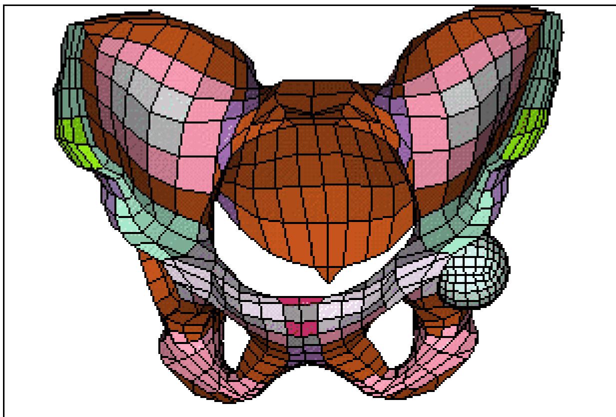

Figure 3a. Simulation of test 9707 : 0 ms.

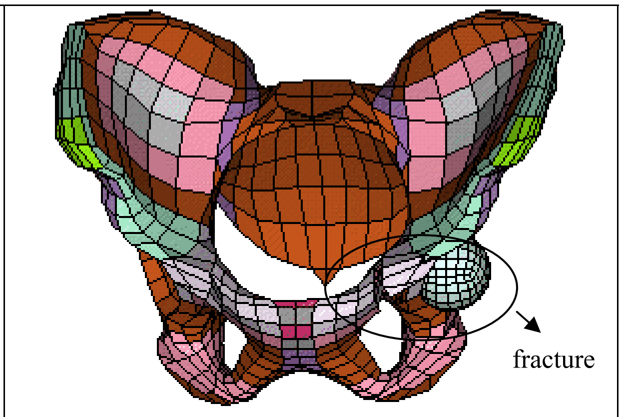

Figure 3b. Simulation of test 9707 : 5 ms.

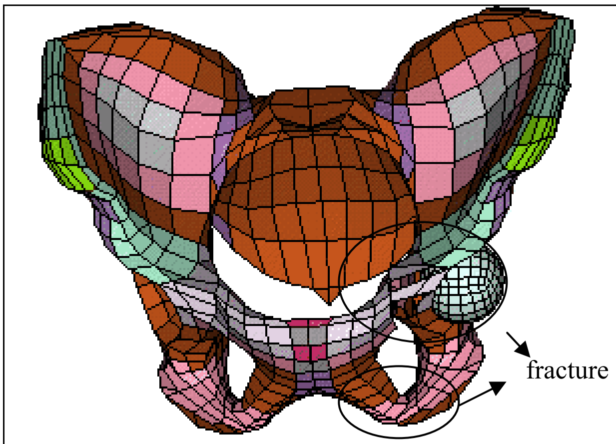

Figure 3c. Simulation of test 9707 : 8 ms.

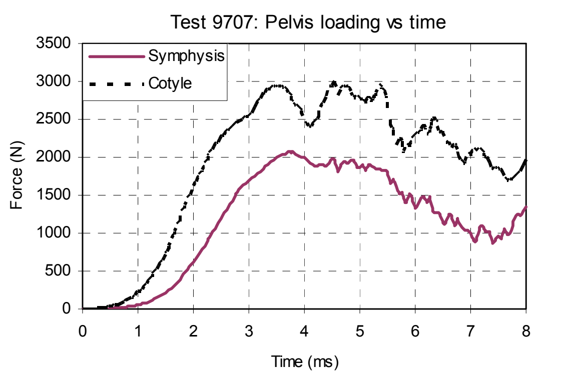

Figure 3d. Cotyle force and symphysis force.

Table 2 summarizes material laws determined by simulating the isolated pelvis tests. Figures in the appendix give a comparison of model responses with experiments. Table 3 summarizes injury outcome of experiments and injury reproduced by models.

Table 2.
Mechanical parameters determined for 11 isolated pelvis bone tested

Tests	E	σy	σmax	εp
9603	11500	57.5	87.5	3%
9604	10000	100	100	3%
9605	50000	250	280	3%
9607	20000	100	130	3%
9701	15000	75	105	3%
9702	29000	145	175	3%
9703	3000	60	60	3%
9704	25000	125	150	0.5%
9705	12000	60	90	3%
9706	30000	150	180	3%
9707	22000	110	140	3%

Table 3.
Injury outcome of experiments and simulation results

	9603	**9604**	**9605**	**9607**
Experiment	Bone fracture	Bone fracture	No bone fracture	Bone fracture
Simulation	Bone fracture	Bone fracture	No bone fracture	Bone fracture
	9701	**9702**	**9703**	**9704**
Experiment	Bone fracture	No bone fracture	Bone fracture	Bone fracture
Simulation	Bone fracture	Bone fracture	Bone fracture	Bone fracture
	9705	**9706**	**9607**	
Experiment	Bone fracture	Bone fracture	Bone fracture	
Simulation	Bone fracture	Bone fracture	Bone fracture	

For a total of eleven tests, nine have been successfully simulated with material laws where:

$\sigma y = 0.005*E$

$\sigma u - \sigma y = 30$ MPa

$\varepsilon p = 3\%$

Material laws determined for tests N9604 and N9703 do not satisfy the relation $\sigma y = 0.005*E$ while one test urged an εp of 0.5%.

Globally we can see that a damageable elastoplastic law with $\sigma y = 0.005*E$, $\sigma u - \sigma y = 30$ MPa, $\varepsilon p = 3\%$ allows representing the majority of pevis bone tested by Guillemot et al.

Establishing relationship between material law and injury risk

Guillemot tests on isolated pelvis bone and its simulation have permitted to have a first estimation of different mechanical parameters. But alone, they do not allow establishing relationship between material laws and probability of pelvic fracture occurrence. One way to achieve this objective is to simulate impactor tests on cadavers. In fact data from this type of tests are the most abundant and cover largely configurations with and without pelvis injuries. Furthermore the test set-up is easy to be duplicated by model, thus avoiding confusion due to error on boundary conditions. Following is a brief description of the most commonly used impactor test configurations on pelvis.

Césari tests – Césari *et al.* [1980, 1982] performed 55 tests on pelvis, using 22 fresh human cadavers. The impactor is 17.3 kg and the impacting system is the portion of a sphere (r = 600 mm, R = 175 mm). The impact speed was increased progressively in order to reach the pelvic fracture at a level as close as possible to the tolerance. However 5 cadavers were fractured at the first impact. Subjects were seated in a low friction surface. The impactor was guided in its impact direction.

Bouquet tests – Bouquet *et al.* [1994, 1998] performed 20 tests on pelvis, using 10 fresh human cadavers. The impactor was 23.4 kg and the impacting system was a flat, rectangular rigid plate (200 x100 mm^2). Each cadaver was impacted firstly at a low speed (around 3.5 m/s) and then at a higher speed (around 6.7 m/s). The subjects were seated in a low friction surface. The impactor was guided in its impact direction.

Iso-energy tests – Bouquet *et al.* [1998] perfomed 11 new cadaver tests on pelvis, using 11 fresh human cadavers. But this time the impactor was a flat, rectangular rigid plate of a larger size (200x200 mm^2). Furthermore the impactor mass (12 and 16 kg) and impact speed (from 9.5 to 13.7 m/s) were disigned in such a way to know the respective role of impactor mass and its velocity for a given level of energy.

Viano tests – Viano [1989] perfomed 14 cadaver tests on pelvis, using 8 unembalmed human cadavers. Impact was realized by a 150 mm flat 23.4 kg pendulum. Impact speeds varied from 3.98 to 10.1 m/s. The cadaver was suspended upright with hands and arms over head.

Injury risk curve in terms of impact force were drawn (see Figure 4) respectively for Césari tests and Bouquet tests. No injury curve was drawn for Viano tests since the number of cases with injury (only 2 cases) are too low . Iso-energy tests contain only 2 cases without injury, too low also to calculate injury risk curve. It can be observed that Césari tests and Bouquet tests lead to very close risk curve.

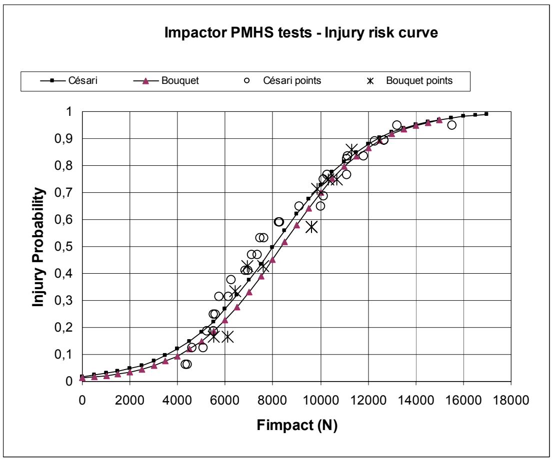

Figure 4. Risk curves on pelvis in terms of impact force according to Césari tests and Bouquet tests.

From these data we can see that:

- 20% of the subjects are exposed to injuries under an impact of 5250 N.
- 50% of the subjects are exposed to injuries under an impact of 8000 N
- 80% of the subjects are exposed to injury under an impact force of 10800.

By simulating Césari tests and Bouquet tests, material laws corresponding respectively to these three levels of tolerance can be determined.

In order to simulate these impactor tests, a human body model was used [Lizée *et al.* 1998]. The pelvis model developed above was integrated to this whole body model. Material laws for pelvis bone were expected to be determined in the variation range of laws given by simulations of Guillemot tests. Figure 5 shows the model set-up for simulation of Césari test configuration.

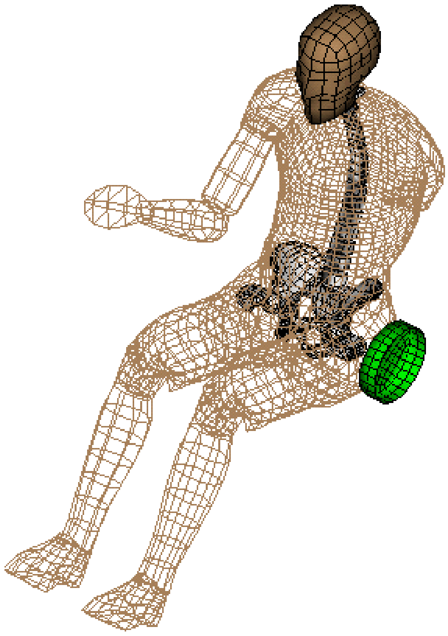

Figure 5. Model set-up for Césari test configuration.

Figure 6 shows results of simulations corresponding to these three levels of loading on pelvis. For each loading level two simulations are presented, one leading to pelvis bone fracture and another not. Table 4 shows material laws used for these simulations. For example no bone fracture was observed with material law Medium-U for an pelvis loading of 8000 N. With a material law slightly less resistant (Medium-L) bone fracture was observed. So we can fix a threshold material law situated between laws Medium-U and Medium-L to represent population with medium resistance. In same way threshold material laws can be defined to represent more fragile and more resistant groups of population. Table 5 gives threshold material laws representing these three groups of population.

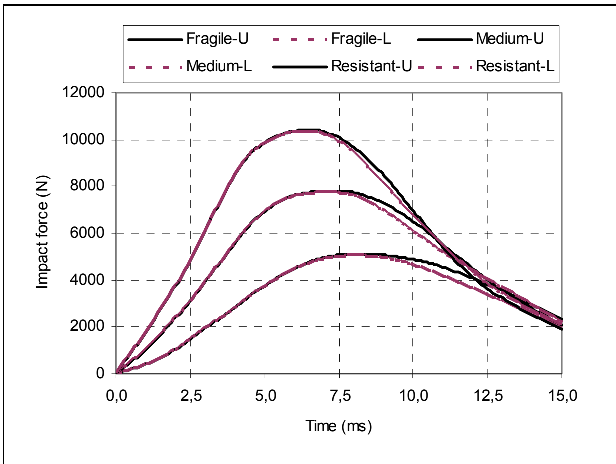

Figue 6a. Impact force time history.

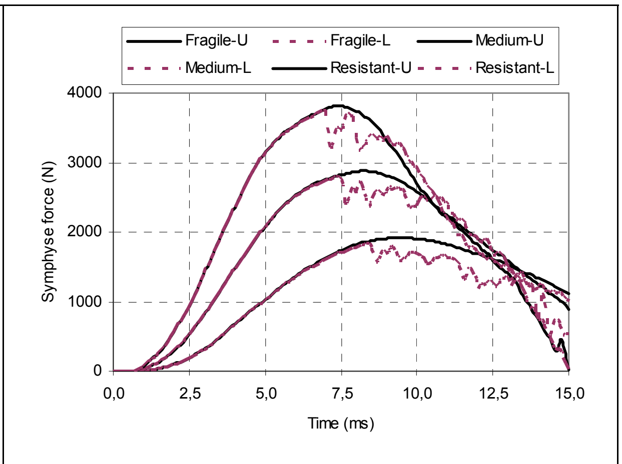

Figure 6b. Symphysis force time history.

Table 4.
Material laws used to identify threshold for each population group (fragile, medium and resistant)

	E	σy	σmax	εp	Fracture
Fragile-L	18000	90	120	3%	Y
Fragile-U	19600	98	128	3%	N
Medium-L	29000	145	175	3%	Y
Medium-U	30000	150	180	3%	N
Resistant-L	40000	200	230	3%	Y
Resistant-U	41000	205	235	3%	N

Table 5.
Material laws representing three population groups (fragile, medium and resistant)

	E	σy	σmax	εp
Fragile	19000	95	125	3%
Medium	29500	147	177	3%
Resistant	40500	202	232	3%

DISCUSSION

It is important to evaluate the relevance of pelvis model to predict forces applied to the pelvis at different impact energy levels. To do this it is essential to select adequate experimental data. One factor to consider is the mass of impacted subject due to its importance for dynamic test, especially when impact velocity is high. Model developed in this study representing a 50th percentile male, it would be misleading to compare it with data affected by the use of cadavers too different from a 50th percentile male in terms of body mass. No evidence showing relevance of existing techniques of normalization, it is preferable to use raw data while eliminating tests performed with subjects too light or too heavy (i.e. not included between 77±10 kg). Age is another influent factor since it is correlated globally with the mechanical resistance of cadaver.

Figure 7 shows characteristics of cadavers used in the experiments listed in the precedent sections.

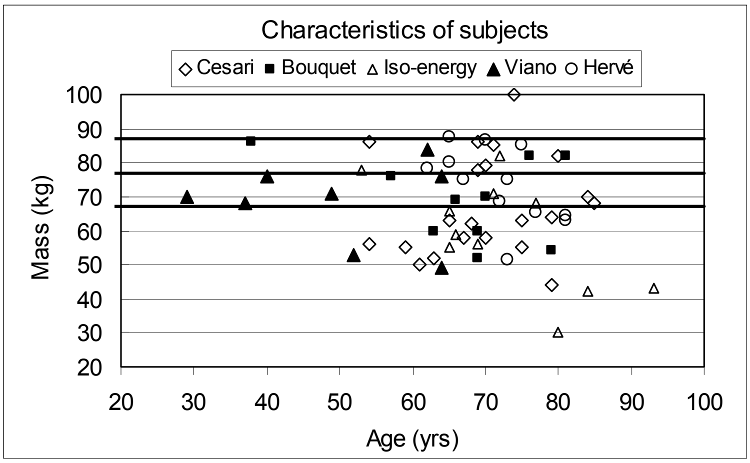

Figure 7. Characteristics of subjects used in different impactor tests.

It can be observed that:

- Among 20 cadavers used in Césari tests, only 7 had a mass between 77kg±10kg. They were only 4 over 11 for iso-energy tests. Subjects used in Bouquet tests and Viano tests were generally closer to the mass of the 50th percentile male.
- Most of subjects tested are old, concentrated between 60 and 80 years.

In the following section, the model responses in terms of pelvis loading and bone fracture are compared to experiments. Only tests performed with subjects with mass between 77kg±10kg were used.

Césari tests - Figure 8 compares impact force between model and experiments. The three material laws used correspond to respectively a fragile bone, a medium bone and a resistant bone. One can observe that model responses are situated on the upper limit of impact force distribution given by experiments.

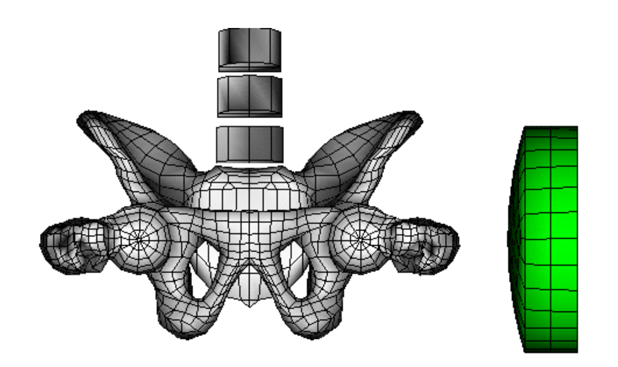

Figure 8a. Zoom of model set-up for Césari configuration.

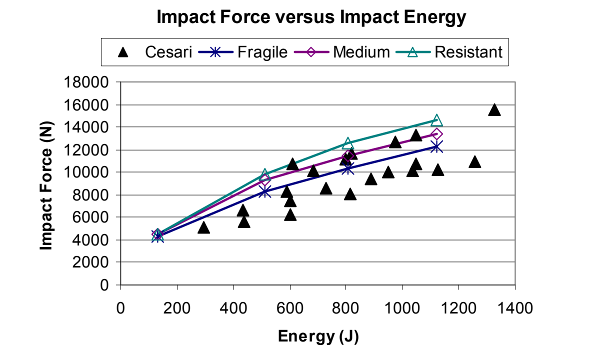

Figure 8b. Comparison of model responses to Césari tests.

Bouquet tests and Viano tests - Since all these tests used an impactor of 23,4 kg, they were combined and examined together. Figure 9 compares impact force between model and experiments. The three material laws used correspond to respectively a fragile bone, a medium bone and a resistant bone. One can observe that pelvis model matches well with Viano tests. However Viano tests showed no injuries for all impact energy while pelvis model fractured even with resistant material law at an impact energy of 1150 J. With respect to Bouquet tests, pelvis model responses are situated in the lower limit of experimental data.

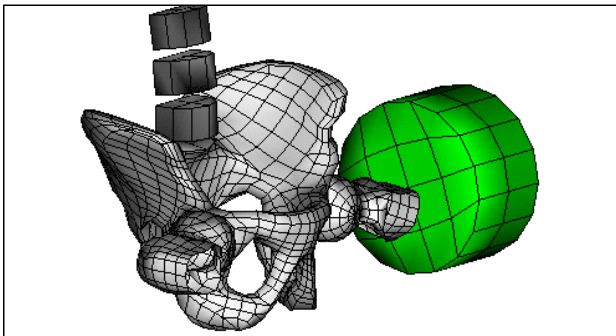

Figure 9a. Zoom of model set-up for Viano configuration.

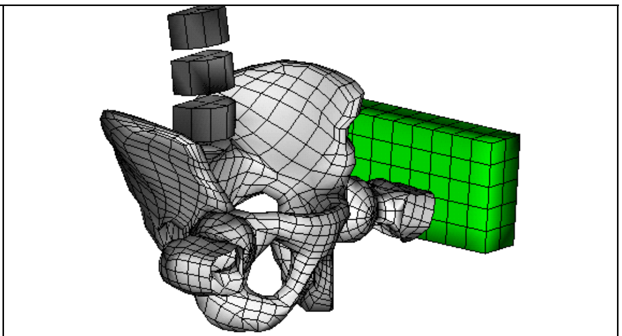

Figure 9b. Zoom of model set-up for Bouquet configuration.

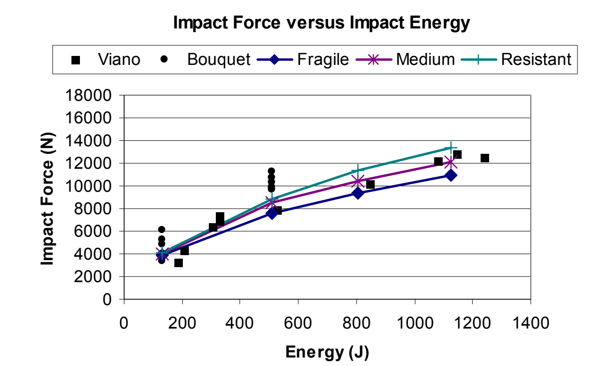

Figure 9c. Comparison of model responses to Viano tests and Bouquet tests.

Iso-energy tests - Figure 10 compares impact force between model and experiments. The three material laws used correspond to respectively a fragile bone, a medium bone and a resistant bone.

One can see that pelvis model shows good responses for high energy. In terms of injury outcome, pelvis model fractured as its experimental counterpart.

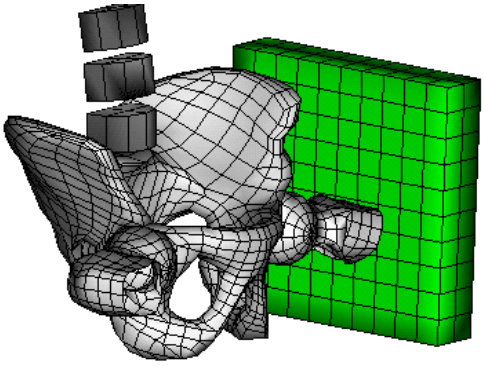

Figure 10a. Zoom of model set-up for Iso-energy configuration.

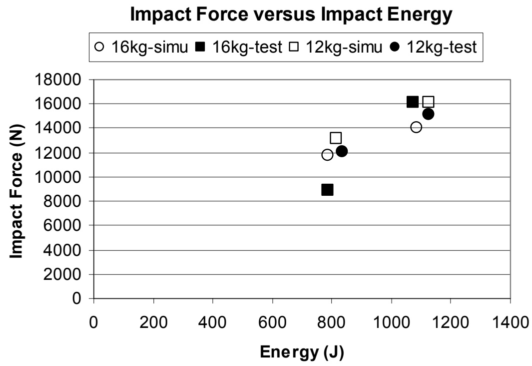

Figure 10b. Comparison of model responses to Iso-energy tests.

Elements presented above show that pelvis model is globally relevant with respect to experiments in terms of pelvis loading prediction, this for a large range of impact energy from 130 to 1150 Joules.

Many experiments on pelvis were also performed under sled configurations. Simulation of these tests is much more difficult than that of impactor tests since test set-up is generally more complex and there are more risks of confusion due to error on boundary conditions. Before undertaking simulations of this type of experiments it is necessary to identify tests with reasonable clarity on boundary conditions and adequate measurements allowing comparison with results of simulations.

CONCLUSIONS

Eleven experiments on isolated pelvis bone under lateral impact have been simulated individually by taking into account proper geometry of each pelvis. These simulations showed that by keeping a constant pelvis cortical bone thickness distribution for all pelvis bones tested and by using a damageable elastoplastic material law, the behavior of these eleven pelvis bones in terms of stiffness and bone fracture can be reproduced by defining an equivalent elastic modulus, a yielding stress and a damage plastic strain. Based on impactor tests on cadavers, a generic pelvis model for a 50th male was defined. Three material laws were associated with this model, representing respectively a fragile, a medium and a resistant pelvis bone. The mechanical behavior of this pelvis model was compared to experimental data of impactor tests on cadaver pelvises. It showed that pelvis model is globally relevant with respect to experiments in terms of pelvis loading prediction, this for a large range of impact energy from 130 to 1150 Joules.

REFERENCES

1. Besnault B., Guillemot H., Robin S., Lavaste F., Le Coz J.Y. (1998) A parametric finite element model of the human pelvis. 42nd Stapp Car Crash Conference. 1998.
2. Bouquet R., Ramet M. (1994) Thoracic and pelvis human responses to impact. Proceeding of ESV1994 Munich.
3. Bouquet R., Ramet M., Bermond F., Caire Y., Talantikite Y., Robin S. and Voiglio E. (1998) Pelvis human responses to lateral impact. Proceeding of ESV1998.
4. Burstein AH et al. (1976) Aging of bone tissue : mechanical properties. J Bone Joint Surg 58(A):82.
5. Césari D. and Ramet M. (1982) Pelvic tolerance and protection criteria in side impact. Proceeding of the 26th Stapp Car Crash Conference, Society of Automotive Engineers, Warrendale, PA.
6. Chamouard F., Bouchard L., Brun-Cassan F., Le Coz JY., Guillon F (1993) Simulation of the human behavior in lateral impact. Proceeding of IRCOBI 1993, Eindhoven, the Neitherlands.
7. Dalstra M., Huiskes R., Odgaard A., Van Erning L.(1993) Mechanical and textural properties of the pelvic trabecular bone. Journal of Biomechanics. 1993 ; 26(4-5). 523-535.
8. Dalstra M. and Huiskes, R. (1995) Load transfer across the pelvic bone, Journal of biomechanics, 28(6), pp. 715-724, 1995
9. Dalstra M., Huiskes, R. and Van Erning, L. (1995) Development and validation of a three dimensional finite element model of the pelvic bone, Journal of biomechanical engineering, 117, pp. 272-278, 1995
10. Dawson J.M., Khmelniker B.V., McAndrew M.P. (1999) Analysis of the structural behavior of

the pelvis during lateral impact using finite element method. Accident Analysis and Prevention. 1999;(31). 109-119.
11. Fung Y.C., Biomechanics - Mechanical properties of living tissues. 1965 ; Bone and cartilage. Springer-Verlag.
12. Goel V.K., Valliapan S., Svensson N.L.(1978) Stresses in the normal pelvis. Comp. Biol. Med. 1978 ; 8 91-104.
13. Guillemot H. (1992) Etude du comportement statique du basin osseux soumis à des efforts latéraux, Mémoire DEA, ENSAM de Paris.
14. Guillemot H., Skalli, W., Lavaste, F, Got, C. and Le Coz, J.Y. (1995) Static behavior of the pelvic bone under side loading conditions, PLEI Conference, Washington, 1995
15. Guillemot H., Besnault, B., Robin, S., Got, C., Le Coz, J.Y., Lavaste, F. and Lassau, J.P. (1997) Pelvic injuries in side impact collisions : an accidental analysis and dynamic tests on isolated pelvic bones, 41th Stapp Car Crash Conference, 1997
16. Krige D.G. : A statistical approach to some basic mine valuation problems on the Witwatersrand, J. Chem. Metall. Min. Soc. S. Afr., 52, pp. 119-139
17. Kuhn J.L., Goldstein S.A., Choi K., London M., Feldkamp L.A. and Matthews L.S. (1989) Comparison of the trabecular and cortical tissue moduli from iliac crests, Journal of orthopaedic research, 7(6), pp. 876-884, 1989
18. Lizee E., Robin S., Song E., Bertholon N., Le Coz J.Y., Besnault B., Lavaste F. (1998) Development of a 3D finite element model of the human body. 42nd Stapp Car Crash Conference. 1998 ; 115 p.
19. Mak A.F. (1986) The apparent visco-elastic behavior of articular cartilage - The contributions from the intrinsic matrix visco-elasticity and interstitial fluid flows. Jouranl of biomechanical engineering. 1986.
20. Oonishi H., Isha H., Hasegawa T. (1983) Mechanical analysis of the human pelvis and its application to the artificial hip joint-by means of the three dimensional finite element method. Journal of Biomechanics. 1983 ; 16(6). 427-444.
21. Plummer J.W., Bidez M.W., Alonso J. (1996) Parametric Finite Element Studies of the Human Pelvis : the Influence of Load Magnitude and Duration on Pelvic Tolerance during Side Impact. STAPP 96. 1996 ; 17 p.
22. Renaudin F., Guillemot H., Lavaste, F. and Skalli, W. (1993) A 3D finite element model of pelvis in side impact, 37th Stapp Car Crash Conference, 1993
23. Reynolds, H., Snow, C. and Young, J. (1981) Spatial geometry of the human pelvis. Memorandum report No AAC-119-81-5
24. Viano D. (1986) Biomechanics of bone and tissue: a review of material properties and failure characteristics. Proceeding of the 30th Stapp Car Crash Conference, pp.33-63, Society of Automotive Engineers, Warrendale, PA
25. Viano D. (1989) Biomechanical responses and injuries in blunt lateral impact. Proceeding of the 33th Stapp Car Crash Conference, pp.113-141, Society of Automotive Engineers, Warrendale, P.

APPENDIX

Model responses compared to isolated pelvis bone tests

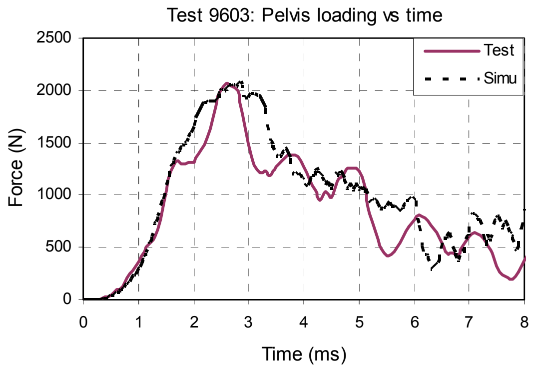

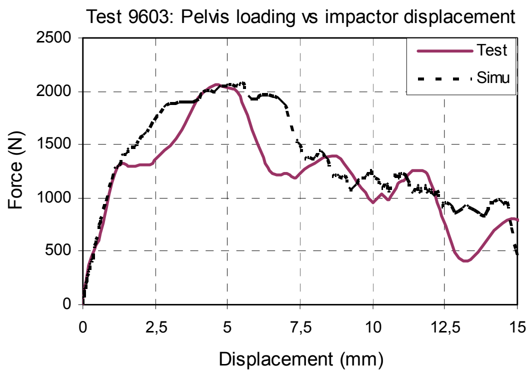

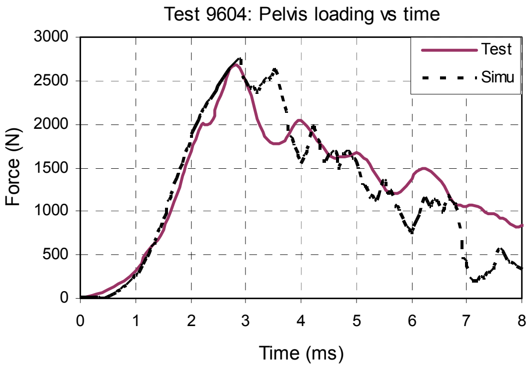
Test 9604: Pelvis loading vs time
Test
Simu
Force (N)
0
500
1000
1500
2000
2500
3000
0
1
2
3
4
5
6
7
8
Time (ms)

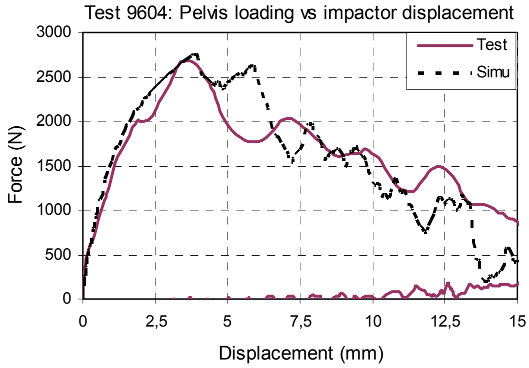
Test 9604: Pelvis loading vs impactor displacement
Test
Simu
Force (N)
0
500
1000
1500
2000
2500
3000
0
2,5
5
7,5
10
12,5
15
Displacement (mm)

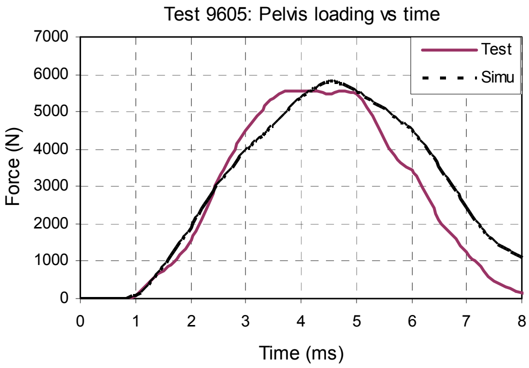
Test 9605: Pelvis loading vs time
Test
Simu
Force (N)
0
1000
2000
3000
4000
5000
6000
7000
0
1
2
3
4
5
6
7
8
Time (ms)

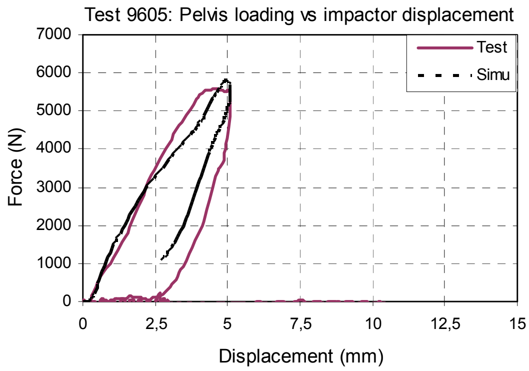
Test 9605: Pelvis loading vs impactor displacement
Test
Simu
Force (N)
0
1000
2000
3000
4000
5000
6000
7000
0
2,5
5
7,5
10
12,5
15
Displacement (mm)

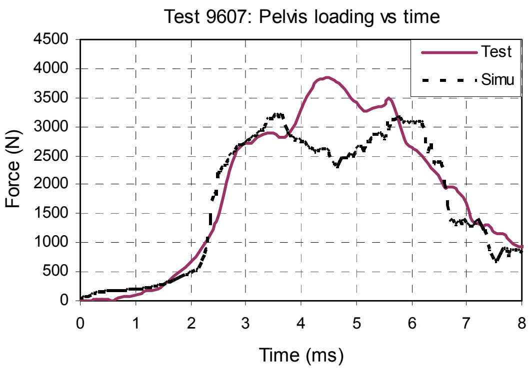
Test 9607: Pelvis loading vs time
Test
Simu
Force (N)
0
500
1000
1500
2000
2500
3000
3500
4000
4500
0
1
2
3
4
5
6
7
8
Time (ms)

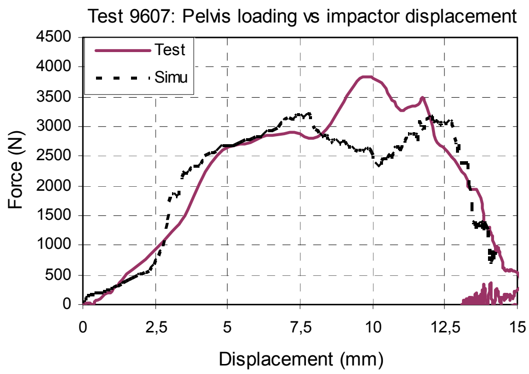
Test 9607: Pelvis loading vs impactor displacement
Test
Simu
Force (N)
0
500
1000
1500
2000
2500
3000
3500
4000
4500
0
2,5
5
7,5
10
12,5
15
Displacement (mm)

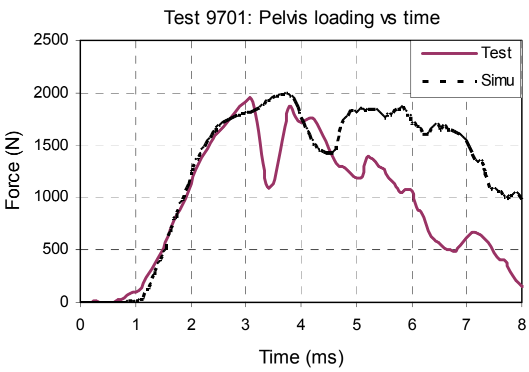
Test 9701: Pelvis loading vs time
Test
Simu
Force (N)
0
500
1000
1500
2000
2500
0
1
2
3
4
5
6
7
8
Time (ms)

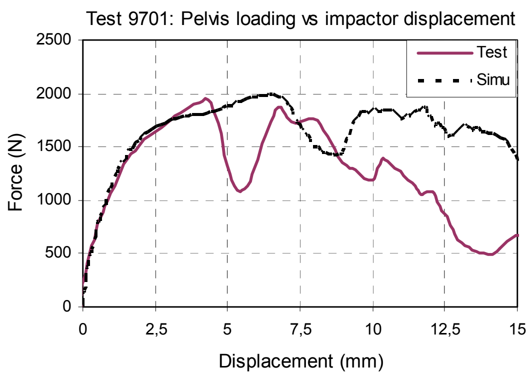
Test 9701: Pelvis loading vs impactor displacement
Test
Simu
Force (N)
0
500
1000
1500
2000
2500
0
2,5
5
7,5
10
12,5
15
Displacement (mm)

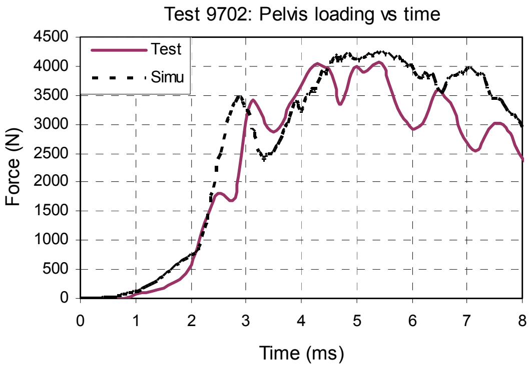
Test 9702: Pelvis loading vs time
Force (N)
Time (ms)
Test
Simu

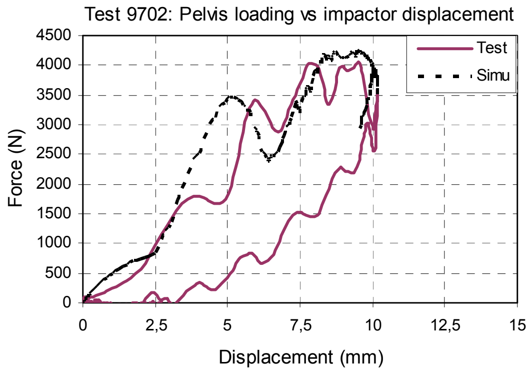
Test 9702: Pelvis loading vs impactor displacement
Force (N)
Displacement (mm)
Test
Simu

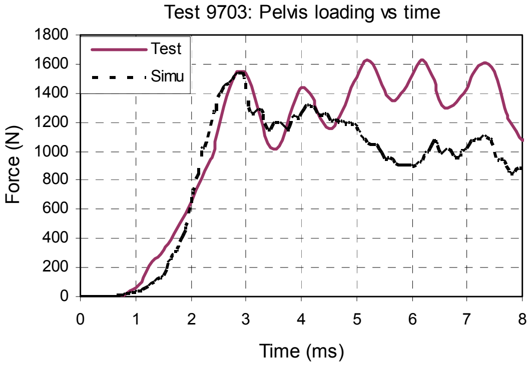
Test 9703: Pelvis loading vs time
Force (N)
Time (ms)
Test
Simu

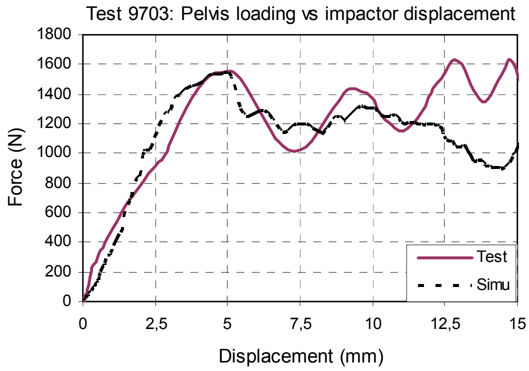
Test 9703: Pelvis loading vs impactor displacement
Force (N)
Displacement (mm)
Test
Simu

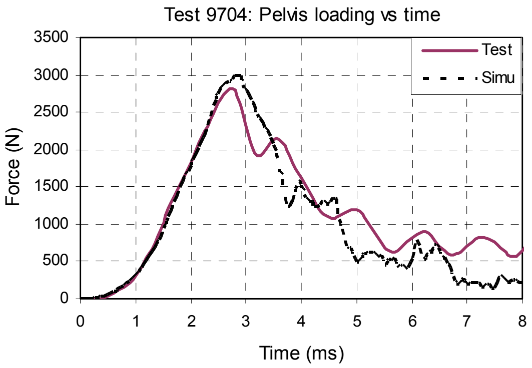
Test 9704: Pelvis loading vs time
Force (N)
Time (ms)
Test
Simu

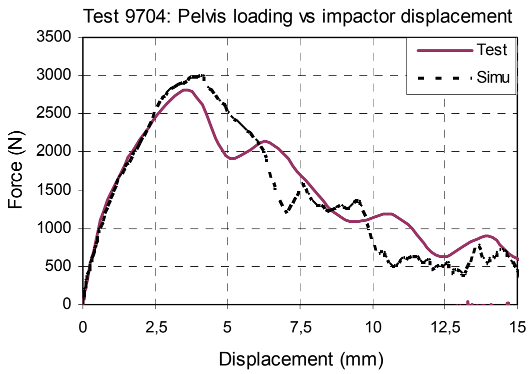
Test 9704: Pelvis loading vs impactor displacement
Force (N)
Displacement (mm)
Test
Simu

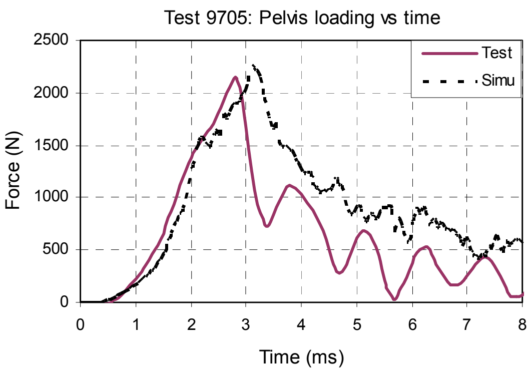
Test 9705: Pelvis loading vs time
Force (N)
Time (ms)
Test
Simu

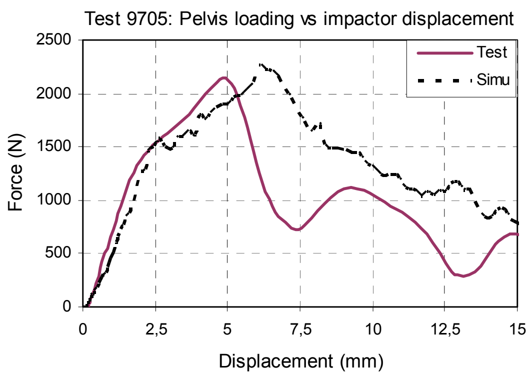
Test 9705: Pelvis loading vs impactor displacement
Force (N)
Displacement (mm)
Test
Simu

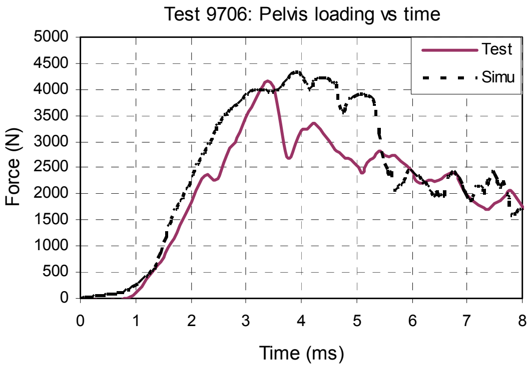
Test 9706: Pelvis loading vs time
Force (N)
Time (ms)
Test
Simu

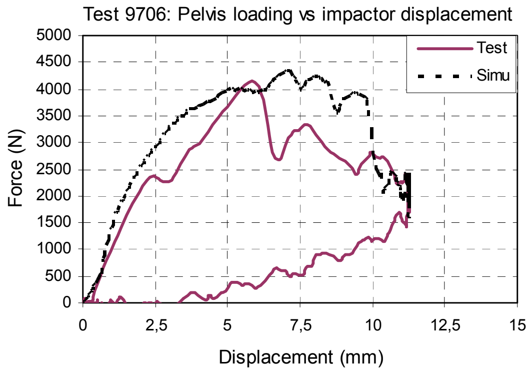
Test 9706: Pelvis loading vs impactor displacement
Force (N)
Displacement (mm)
Test
Simu

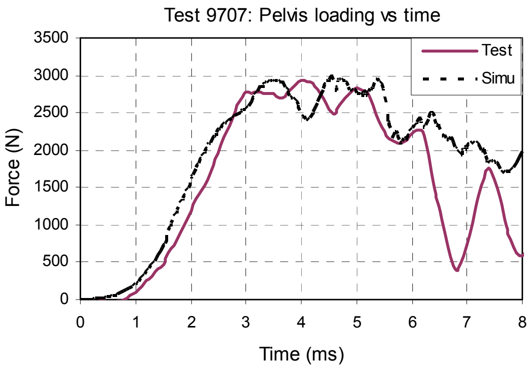
Test 9707: Pelvis loading vs time
Force (N)
Time (ms)
Test
Simu

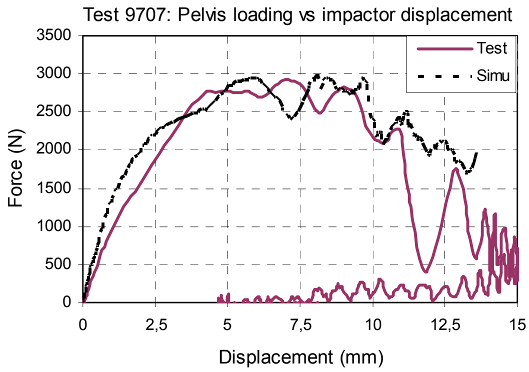
Test 9707: Pelvis loading vs impactor displacement
Force (N)
Displacement (mm)
Test
Simu